PROCEEDINGS, 47th Workshop on Geothermal Reservoir Engineering
Stanford University, Stanford, California, February 7-9, 2022
SGP-TR-223

The Geothermal Geodometer: A Geochemical Approach to Targeting Upflow in Long Valley

Adam Johnson, Robert Selwood, and Daniel Feucht

Ormat Technologies, 6140 Plumas St, Reno, Nevada, USA

rselwood@ormat.com

Keywords: Long Valley geothermal field, Casa Diablo, Basalt Canyon, geothermometry, geodometer, upflow, outflow, lidar, magnetotellurics

ABSTRACT

The Long Valley Caldera complex located on the eastern slope of the Sierra Nevada hosts a productive geothermal system on the southwest margin. Power generation from the field harnesses 150-190°C fluids from outflow in the Basalt Canyon and Casa Diablo areas. This outflow extends a further 10km to the east of Casa Diablo and is expressed by surface manifestations such as fumaroles, mud pots, and hot springs with indicated resource upflow temperatures approaching 240°C based on chemical geothermometers. These estimated temperatures greatly exceed maximum measured temperatures and conjunction with historic drilling suggest a higher temperature upflow to the west.

Chemical geothermometers from several wells and surface features along the outflow path were used to back-calculate a distance-to-upflow from the current Basalt Canyon production wells. General trends show an overall linear decrease in temperatures from west to east and a more rapid re-equilibration of silica relative to cation geothermometers, both of which are consistent with previous studies and our understanding of reaction kinetics. When quartz geotemperature is plotted as a function of distance from the westernmost, highest temperature sample (production well 14-25), extrapolation to inferred resource temperatures of 230-240°C suggests that upflow occurs within a 5-7.5 km radius from that point.

Previous geophysical and structural studies have suggested upflow may be associated with permeability along high angle faults that form the western moat, which falls within the 5-7 km target area. Upflow in this area is further supported by resistivity structures in 3D modelled magnetotelluric data and lidar data that indicates a WNW structural pathway linking this area with production in Basalt Canyon. This chemical "geodometer" approach shows the utility of applying this technique to understanding geothermal systems that produce exclusively from outflow and can provide insight into additional exploration drilling or geophysical studies to further develop higher temperature resources.

1. INTRODUCTION

The geothermal system is located in the Long Valley Caldera, on the southwest margin of a rhyolitic resurgent dome complex (Hildreth, 2017a). The distribution of thermal manifestations (fig.1) and measured temperature profiles from wells within the field illustrate a general west to east outflow path manifest at surface over approximately 15km strike length. Production occurs over a 5km strike within two areas along this outflow path at Basalt Canyon in the west and Casa Diablo in the east (fig. 4) with maximum production temperatures of 190°C and 150°C respectively. East of this numerous thermal springs occur at surface above low temperature/sub economic outflow with fluid chemistries indicative of the reservoir.

The location of upflow remains unknown, despite several attempts to intersect it with drilling (Benoit, 1984; Sorey et al, 1991). Fluid chemistries of wells from Basalt Canyon indicate an upflow temperature of 230-240°C based on cation geothermometry. Geothermometry based on production well samples in Casa Diablo and thermal spring samples further east along the Hot Creek, show a trend towards lower temperatures in the distal outflow. This led to the question, can we measure distance traveled by fluid in outflow based on geochemical changes in resource chemistry using the relationships between conductive cooling and re-equilibration of geothermometers as a function of distance? Furthermore, can that 'Geodometer' be used to estimate distance to upflow?

This paper presents an updated conceptual model for upflow based on the re-equilibration of geothermometers along outflow in the context of new structural mapping from lidar, reinterpretation of published 3D magnetotelluric modelling, thermal gradients from historic drilling, and the distribution of young volcanic units.

2. GEOLOGIC SETTING

The known portions of the geothermal system are located on the south and west margins of the Long Valley Caldera, a ~22 by 12 km oval-shaped area of deep structural subsidence formed from the eruption of the Bishop Tuff around 767 ka (fig. 1). This initial eruptive event forms the basal unit of the volcanic sequence which hosts the geothermal system (Hildreth, 2017a). Between 750-640 ka about 40 post caldera eruptions occurred in the central west portion of the caldera forming a resurgent dome complex of rhyolite (Hildreth, 2017a). The current geothermal production area (fig. 1) is located on the southwest margin of this resurgent dome complex which forms the upper sequence of volcanic units that host the geothermal system.

The caldera is structurally located at a stepover between the Hartley Springs and Hilton Creek normal faults that mark the eastern margin of the Sierra Nevada (fig. 1). These faults are linked by a series of N-NW trending normal faults that crosscut the resurgent dome complex and Western moat forming a series of horst and graben structures that control permeability within the geothermal system at large. Estimations of stress from borehole break outs and earthquake focal mechanism inversions (Prejean, 2002) around the production area indicate minimum horizontal stresses (Sh_{min}) are oriented along NE-SW to E-W trends, broadly perpendicular to the N-NW linking structures through this area. A localized seismogenic zone coincident with the south moat suggests that right lateral slip between the Harley Springs and Hilton Creek faults might be accommodated by WNW-ESE trending faults parallel to the buried ring fracture of the Caldera described by (Hildreth, 2017b)

High temperature brines are produced from a lateral body of outflow ranging in temperature from 190°C and 150°C which extends through the Basalt Canyon and Casa Diablo areas to the east (fig. 1). Drilling west of the production area intersected increasing temperature gradients observed in PLV-1 (Benoit, 1984) and a maximum temperature of 218°C associated with a deep inversion in 44-16 (Suemenicht, 1987). This has led several workers to suggest upflow occurs within the western moat of the caldera (Suemenicht, 1987; Blackwell, 1985; Sorey et al, 1991), thought the exact location of the reservoir remains unknown. These areas are associated with numerous young volcanic units ranging from the 150-100 ka rhyolite domes and flows in the Western Moat Coulee, extra-caldera trachybasalt and trachydacite volcanism that formed Mammoth Mountain between 230 and 8 ka, and the 0.6 ka Mono-Inyo rhyolites volcanic chain of domes and flows that extend towards Mono Basin 20 km to the north.

In support of this western upflow model geophysical studies have previously identified locations in the Western Moat and proximal to Mammoth Mountain as potential areas for upflow. Three-dimensional (3D) inversion of broadband magnetotelluric (MT) data by Peacock et al. (2016) revealed a steeply dipping low resistivity feature beneath Inyo Craters that was interpreted as the main conduit for hydrothermal upflow (fig. 5). This sub-vertical feature was interpreted as fracture permeability that appears as a conductor due to the presence of high-temperature saline fluids and low resistivity hydrothermal alteration minerals. Alternatively, given the young age of volcanism and the presence of active fumaroles on Mammoth Mountain (fig. 4) it has been suggested that electrical conductors in this area may indicate the location of hydrothermal upflow (Cumming, 2005).

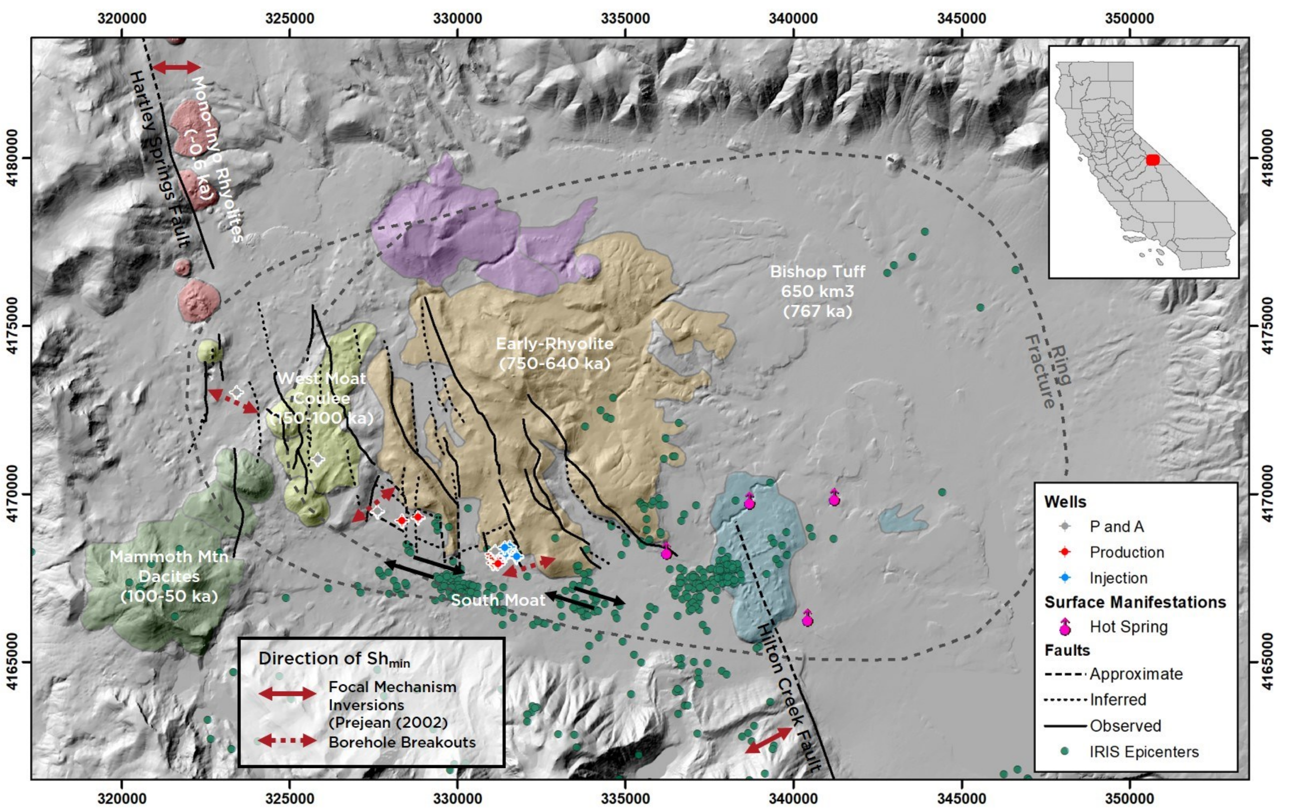

Figure 1: Summary map of the Long Valley Caldera showing the distribution of post caldera eruptions (after Hildreth, 2017a) and major N-NW trending normal faults that crosscut the western and southern portions of the Caldera. Local stress indicators from Prejean (2002) are shown as red arrows parallel to the minimum horizontal stress (Shmin). Geothermal wells are denoted by colored dots and crosses, red (production) and blue (injection) markers occur in the primary production areas. Select hot springs areas considered in this study are shown along the outflow path to the east.

3. METHEDOLOGY

3.1 Geochemical Data

Extensive geochemical datasets exist for the Long Valley Caldera, spanning several decades worth of exploration and production history. The data cover a spatial area of several square kilometers of geothermal activity from the western portion of the caldera eastward along the hydrologic gradient (fig 5). Geochemical datasets used for this study include individual datasets published from literature (Waring, 1965; Mariner, 1976; White, 1990; Sorey, 1991), publicly available data from the United States Geological Survey (URL; https://waterdata.usgs.gov/ca/nwis), and internal company datasets. Samples included geochemical analyses from surface thermal manifestations, well discharges collected during field development, shallow monitoring wells, and production brine collected from pumped wells during normal plant operation. Samples were screened for location along hydrologic gradient, data quality, and by evidence for non-conductive cooling mechanisms. Sample locations with multiple datapoints were averaged unless there was evidence for long-term temporal variability in the dataset that would indicate a change in the resource chemistry. Ambiguous or outlier samples were re-sampled in October 2020 with a series of control points to confirm or refute data quality issues and confirm historical analyses. The final dataset included a total of 61 datapoints and spanned a surface distance of over 10 km. Sample locations and distances used in this study were collected using Google Earth based on provided sample coordinates and are straight-line distances between 14-25 and individual sample locations.

3.2 Geothermometry and The Geodometer

Geothermometry calculations from the geochemical dataset included conductive quartz (T_{qtz}) and uncorrected sodium-potassium-calcium (T_{nkc}). Results showed positive relationship between the two geothermometers ($R^2 > 0.9$) and a slope greater than one, consistent with more rapid re-equilibration of silica versus cation geothermometers with response to temperature, with the hottest temperatures predicted up hydrologic gradient (Basalt Canyon) and decreasing downgradient (Fig. 2). Silica geothermometer results were then plotted as a function of distance from the most western datapoint, well 14-25 in Basalt Canyon, and a linear regression through the resulting dataset. The relationship showed an $R^2 > 0.8$ and was used to predict the estimated additional distance needed for fluid to travel to have cooled from the deep resource temperatures predicted from both cation and isotope geothermometers to those temperatures observed at 14-25 (Fig. 3).

3.3 Structural Data

In 2017 a lidar data set covering 67 km^2 was acquired by Ormat to support mapping efforts. High resolution hill shade maps were produced to help map the distribution of lithologic units and structure. These data have been compared with previous mapping by Hildreth and Fierstein (2016) and Bailey (1989) to produce a revised structural map of Rhyolite Plateau and the Western Moat.

Recent drilling in Basalt Canyon has allowed for the collection of Formation MicroScanner Imagery (FMI) in wells 14-25 and 47-25. From these data, drilling induced tensile fractures were interpreted using WellCAD™ downhole logging software to estimate the local maximum and minimum horizontal stress. The results of this work are presented below in the context of the regional stress state mapped by Prejean (2002) to highlight possible fluid pathways that link the Western Moat and production in Basalt Canyon.

4. RESULTS AND DISCUSSION

4.1 Geodometer

The application of chemical geothermometry to geothermal exploration and development is well established and its ability to help delineate subsurface temperatures and processes affecting the reservoir have been well documented. Oftentimes, observed differences exist between predicted temperature of silica and alkali or isotope-based geothermometers, allowing insight into delineating conductive cooling, boiling, or fluid mixing versus potential deep resource and/or upflow temperatures, with differences attributed to differences in the equilibrium rate constants between the methodologies. This study utilizes changes in silica concentration due to conductive cooling along the known outflow path to predict the distance to upflow from the closest sample point to that upflow.

Geothermal production from Long Valley is confined to the Bishop Tuff and Early Rhyolite geologic units in the outflow path of the system, producing high temperature (150-190°C) brine matched by silica geothermometry. However, both cation and isotope based geothermometers suggest temperatures up to 230-240°C within the system. Data from this study were plotted as a function of T_{qtz} versus distance from the most western datapoint, well 14-25 in Basalt Canyon, extending over ten kilometers through the production zone in Casa Diablo through surface manifestations along outflow and terminating in Hot Creek and the Whitmore Hot Spring complex (Fig. 3). Outliers to the trend are thought to be structurally isolated in the system (66-25), are low-temperature springs with minor geothermal input (Whitmore Hot Springs) or fall in a temperature range where subsurface temperatures are likely more reflective of equilibrium with chalcedony than quartz (Crab Cooker). Regressions through this dataset allow extrapolation of this cooling trend from a starting point at 14-25 to the estimated resource temperature of 230-240°C. Based on this regression, the necessary distance required for fluid travel to reflect the chemistry seen at Basalt Canyon is 5-7 km. This provides a search radius that significantly reduces the area where upflow may be situated and allows integration or targeting of additional geologic and geophysical datasets to provide a higher confidence estimate of higher temperatures within the resource.

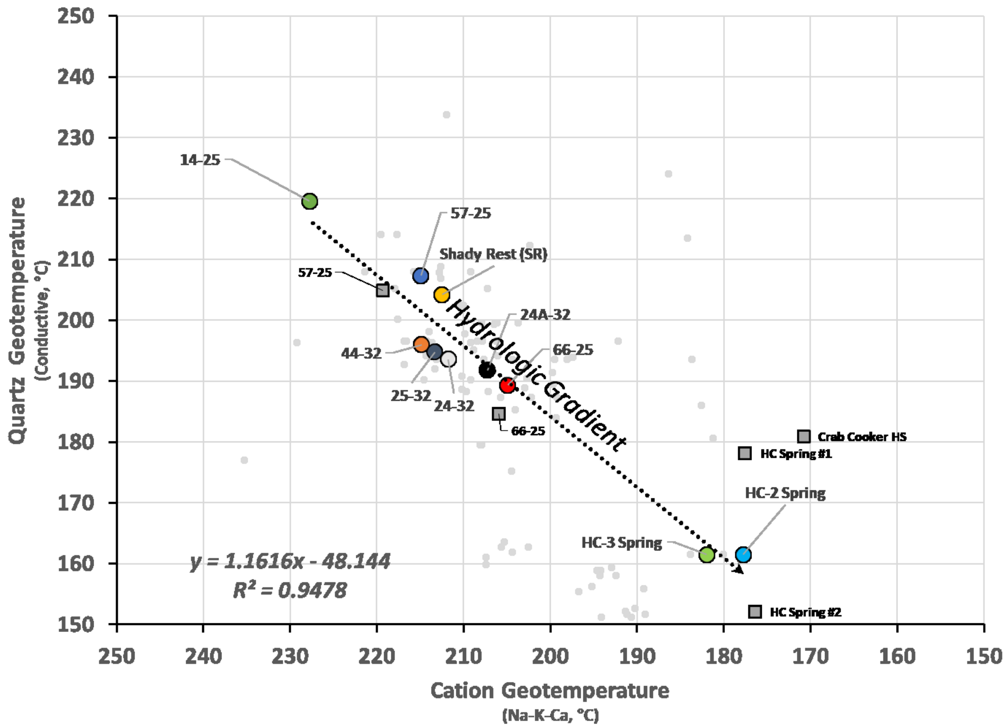

Figure 2: Bivariate plot of Na-K-Ca vs Quartz conductive geothermometers for production wells and hot springs samples along the outflow path. All samples are shown as grey dots, averages for wells and springs are highlighted as colored circles. Grey squares represent sample points collected in Fall 2020

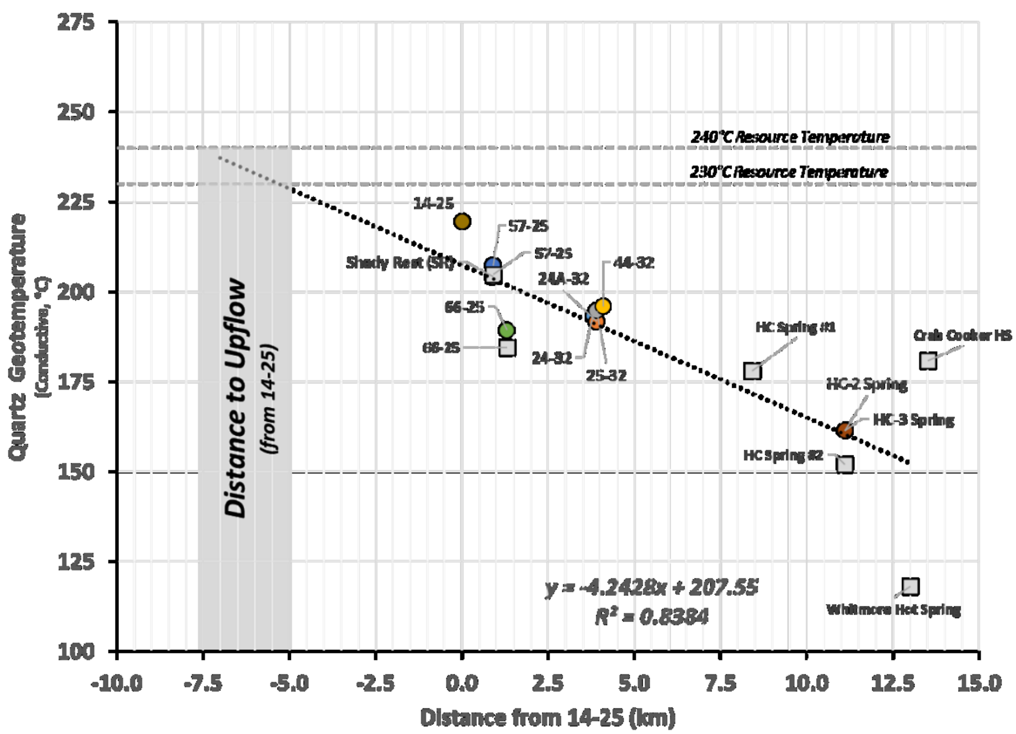

Figure 3: Quartz geotemperature plotted as a function of distance from 14-25 showing a strong linear trend between samples along outflow and distance travelled. Extrapolation towards Na/k and Na-K-Ca temperature estimates suggests upflow is 5-7.5 km up gradient

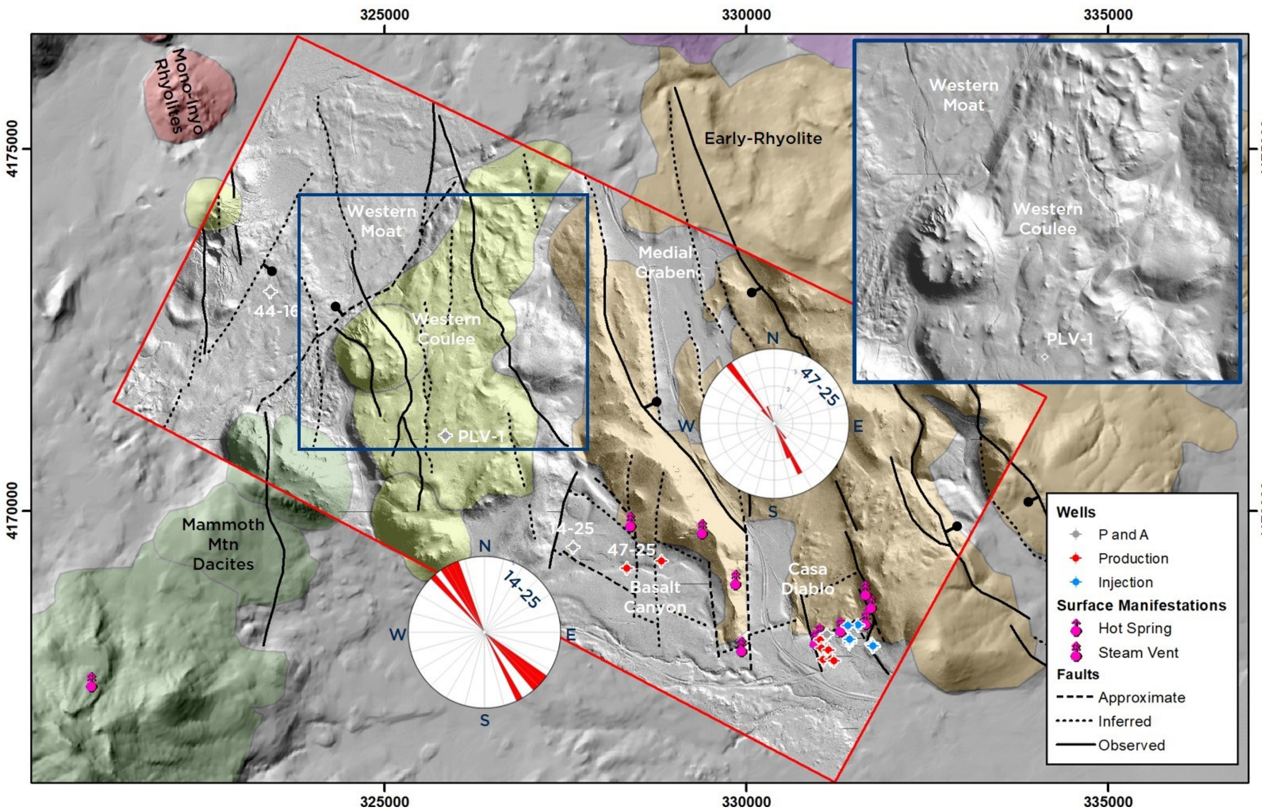

Figure 4: Lidar hill shade map (red insert) with interpreted fault traces. Northwest striking Holocene faults mapped with lidar (fault scarps shown in blue insert) connect the Western Moat to Basalt Canyon. Rose diagrams of imaged tensile fractures in 14-25 and 47-25 indicate NW structures likely represent dilated fluid pathways.

4.2 Fluid Pathways

The distribution of thermal manifestations (fig. 4) and measured temperature profiles from wells within the field illustrate a general west to east outflow path manifest at surface in Basalt Canyon and Casa Diablo by the presence of fumaroles and associated acid sulfate alteration. These thermal manifestations are commonly coincident with permeable fluid pathways and can be correlated to primary feeds zones in both production and injection wells by combined interpretation of FMI data and surficial mapping. Primary feed zones in two Basalt Canyon production wells, 14B-25 and 47-27 (both drilled in 2021), result from structures orientated along a NW and SE strike, broadly parallel with drilling induced fractures in each respective well (fig. 4).

No active thermal features are observed west of production well 14-25 within the Western Coulee and Western Moat, limiting our ability to map permeable structures at surface. However, lidar data over the area highlight a series of NW striking Holocene faults scarps (fig. 4) that have previously not been identified in mapping by Hildreth and Fierstein (2016) and Bailey (1989). These structures are oriented perpendicular to the inferred Sh_{min} based on tensile fractures in 14-25 and 47-25 and therefore are likely to be dilated. These NW oriented structures represent a potential direct fluid pathway connecting upflow within the western moat as indicated by the geodometer to outflow observed to the east.

4.3 Resistivity Structure of Upflow

Geophysical studies of Long Valley have previously identified the Western Moat as an area of the caldera that may host hydrothermal upflow. Three-dimensional (3D) inversion of broadband magnetotelluric (MT) data by Peacock et al. (2016) revealed a steeply dipping low resistivity feature beneath Inyo Craters that was interpreted as the main conduit for hydrothermal upflow. This sub-vertical feature was interpreted as fracture permeability that appears as a conductor due to the presence of high-temperature saline fluids and low resistivity hydrothermal alteration minerals. This feature can be seen in an elevation slice through the 3DMT model at 600 m.a.s.l. as a circular region of low resistivity due north of well 44-16 (fig. 5)

A similar low resistivity feature can also be seen in the 3DMT model beneath Mammoth Mountain (fig. 5). Given the young age of volcanism and the presence of active fumaroles on Mammoth Mountain it has been suggested that this electrical conductor may indicate the location of hydrothermal upflow (Cumming, 2005). Peacock et al. (2016), alternatively, interpreted the Mammoth Mountain anomaly as an isolated body of fluids and gases derived from a deeper zone of partial melt. Although the exact location of this feature is poorly constrained by the distribution of MT stations, it does lie within the radius of upflow estimated by the geodometer.

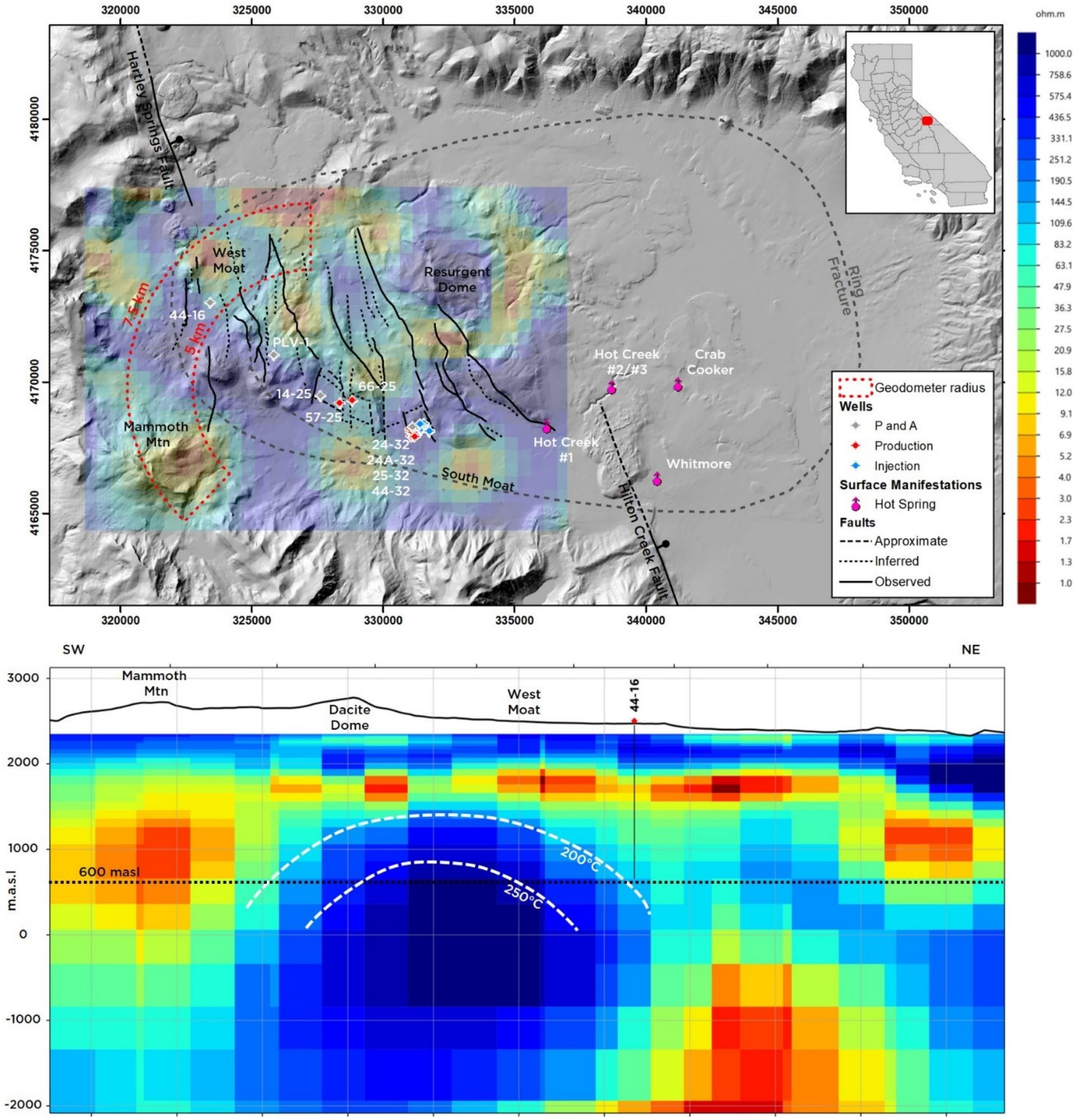

Figure 5: Evidence for hydrothermal upflow in the 3DMT model from Peacock et al. (2016) in (above) map view and (below) cross section. A map view elevation slice through the MT model at 600 meters above sea level shows two conductive features within the geodometer radius that have previously been interpreted as geothermal upflow. Meanwhile, a cross section view along the 5 km geodometer radius reveals a more complex resistivity structure that is typical of economic high-temperature geothermal reservoirs, specifically an up-doming resistor beneath a thin low resistivity clay cap.

Our preferred interpretation of the 3DMT model places the upflow between the two previously identified zones of low resistivity. Extracting a cross section through the 3DMT model along a profile that follows the geodometer radius of 5 km (fig. 5) reveals an up-doming resistor beneath the Dacite Dome. This resistor is capped by a shallow, thin layer of low resistivity, creating a pattern in the electrical resistivity structure matching that of other high-temperature geothermal reservoirs around the world (e.g., Bertrand et al., 2013; Cumming and Mackie, 2010; Arnason et al., 2000). The interpretation of this resistivity structure is that the MT images a transition in hydrothermal alteration from lower temperature, low resistivity clay on the margins of the geothermal reservoir (e.g. smectite), to higher temperature, high resistivity clay within the core of the reservoir (i.e. chlorite). This preferred interpretation is influenced in part by previous experience in exploring and developing high temperature geothermal systems. Further geologic, geophysical, and geochemical analysis, likely including exploratory drilling, will ultimately be required to confirm the location of geothermal upflow within the Western Moat.

5. CONCLUSION

While maximum temperatures of 218°C (44-16) and high temperatures gradients up to 75°C/100m (PLV-1) indicate the presence of a high temperature reservoir west of current production in Basalt Canyon the exact location of this upflow has yet to be intersected. Cation geothermometry from the least re-equilibrated fluid samples (14-25) indicate temperatures between 230°C and 240°C may exist in upflow. A strong correlation between quartz and cation geotemperatures along the outflow path allow estimates of distance to upflow by plotting T_{qtz} as a function of distance from 14-25. Based on this chemical geodometer we estimate upflow between 5 and 7.5 km from 14-25, which correlates with the young volcanism associated with the Mono-Inyo volcanic chain, the Western Moat, and Mammoth Mountain. Analysis of 3DMT modelling and lidar data provide the basis for an updated conceptual model of the Long Valley hydrothermal system that places upflow within the Western Moat 3-4km NE of Mammoth Mountain.

REFERENCES

Árnason, K., Karlsdóttir, R., Eysteinsson, H., Flovenz, O.G., and Gudlaugsson, S.Th. (2000). The resistivity structure of high-temperature geothermal systems in Iceland, Proceedings of the World Geothermal Congress 2000, Kyushu-Tohoku, Japan, 923-928.

Bailey, R. (1989) Geologic Map of Long Valley, Mono-Inyo Craters Volcanic Chain, and Vicinity, Eastern California. U.S. Geological Survey Miscellaneous Investigations Map I-1933.

Benoit, W. (1984) Initial Results from Drillholes PLV-1 and PLV-2 in the Western Moat of the Long Valley Caldera: Geothermal Resource Council, Transactions, 8, 397-402.

Bertrand, E.A., Caldwell, T.G., Hill, G.J., Bennie, S.L., and Soengkono, S., (2013) Magnetotelluric imaging of the Ohaaki geothermal system, New Zealand: Implications for locating basement permeability, Journal of Volcanology and Geothermal Research, 268, 36-45.

Cumming, W., (2005) Targeting geothermal wells in the Rhyolite Plateau Exploration Area based on an updated resource conceptual model. Proprietary Report to Robert Sullivan, Mammoth-Pacific Limited Partnership. 2005-12-18.

Cumming, W., and Mackie, R. (2010) Resistivity Imaging of Geothermal Resources Using 1D, 2D and 3D MT Inversion and TDEM Static Shift Correction Illustrated by a Glass Mountain Case History, Proceedings of the World Geothermal Congress 2010, Bali, Indonesia.

Hildreth, W. (2017a) Fluid-driven uplift at Long Valley Caldera, California: Geologic perspectives, Journal of Volcanology and Geothermal Research, 341, 269–286.

Hildreth, W. (2017b) Concealed Ring-Fault of Long Valley Caldera. In: Hildreth, W. and Fierstein, J., 2017, Geologic field-trip guide to Long Valley Caldera, California: U.S. Geological Survey Scientific Investigations Report 2017–5022–L, 90-98.

Hildreth, W., and Fierstein, J. (2016) Eruptive History of Mammoth Mountain and its Mafic Periphery, California. U.S. Geological Survey Professional Paper 1812, 128 p., 2 plates, scale 1:24,000

Mariner, R.H., et al. (1976). Geochemistry of Thermal Waters in Long Valley, Mono County, California. Journal of Geophysical Research. 81(5), 792-800.

McKenzie, W.F., Truesdell, A.H. (1977). Geothermal Reservoir Temperatures Estimated from the Oxygen Isotope Compositions of Dissolved Sulfate and Water from Hot Springs and Shallow Drillholes. Geothermics. 5(1-4), 51-61

National Water Information System. https://waterdata.usgs.gov/ca/nwis

Peacock, J.R., Mangan, M.T., McPhee, D., and Wannamaker, P.E. (2016), Three-dimensional electrical resistivity model of the hydrothermal system in Long Valley Caldera, California, from magnetotellurics, Geophysical Research Letters, 43(15), doi: 10.1002/2016GL069263.

Prejean, S. (2002) The Interaction of Tectonic and Magmatic Processes in the Long Valley Caldera, California. Stanford University

Shevenell, L., et al. (1987). Chemical and isotopic characteristics of thermal fluids in the Long Valley Caldera lateral flow system, California. In: Transactions. GRC Annual Meeting; 10/11/1987; Sparks, NV. Sparks, NV: Geothermal Resources Council, 195-201

Sorey, M.L., Suemnicht, G.A., Sturchio, N.C. and Nordquist, G.A., (1991). New Evidence on the Hydrothermal System in Long Valley Caldera, California, From Wells, Fluid Sampling, Electrical Geophysics, and Age Determinations of Hot-Spring Deposits. Journal of Volcanology and Geothermal Research. 48(3-4), 229-263.

Suemnicht, G. (1987) Results of Deep Drilling in the Western Moat of Long Valley, California: Eos, 68 (40), 784-798.

Taylor, B.E., Gerlach, T.M. (1983). Chemical and Isotopic Composition of Casa Diablo Hot Spring: Magmatic CO2 near Mammoth Lakes, CA. EOS, Transactions; 02/1983: American Geophysical Union,. 58

Waring, G.A., (1965). Thermal Springs of the United States and Other Countries of the World - A Summary. Washington, D.C.: United States Government Printing Office. Report No.: Professional Paper 492.

White, A.F., et al. (1990). Sources and Fractionation Processes Influencing the Isotopic Distribution of H, O and C in the Long Valley Hydrothermal System, California, U.S.A. Applied Geochemistry. 5(5-6), 571-585.